

# Landing of size-selected $\text{Ag}_n^+$ clusters on single crystal $\text{TiO}_2$ (110)-(1×1) surfaces at room temperature

Lauren Benz, Xiao Tong, Paul Kemper, Yigal Lilach, Andrei Kolmakov, Horia Metiu, Michael T. Bowers, and Steven K. Buratto<sup>a)</sup>

*Department of Chemistry and Biochemistry, University of California, Santa Barbara, California 93106*

(Received 9 December 2004; accepted 22 December 2004; published online 14 February 2005)

Mass-selected  $\text{Ag}_n^+$  ( $n=1, 2, 3$ ) clusters with impact energy less than 2 eV per atom were deposited from the gas phase onto rutile titania (110)-(1×1) single crystal surfaces at room temperature and imaged using ultra-high vacuum scanning tunneling microscopy. Upon reaching the surface, Ag monomers sintered to form three-dimensional islands of approximately 50 atoms in size, with an average measured height of 7.5 Å and diameter of 42 Å. This suggests that the monomers are highly mobile on the titania surface at room temperature. Dimers also sintered to form large clusters upon deposition, approximately 30 atoms in size, with an average height of 6.2 Å and diameter of 33 Å. Clusters formed from monomer deposition appeared approximately three times more frequently at step edges than clusters formed from dimer deposition, indicating that the surface mobility of deposited monomers is higher than that of deposited dimers. In sharp contrast to the deposition of monomers and dimers, the deposition of trimers resulted in a high density of very small clusters on the order of a few atoms in size, indicative of intact trimers on the surface, implying that deposited trimers have very limited mobility on the surface at room temperature. © 2005 American Institute of Physics. [DOI: 10.1063/1.1859271]

## INTRODUCTION

The discovery that nanoclusters of Au and Ag on oxide supports catalyze many reactions, including the oxidation of CO and small olefins<sup>1-4</sup> has stimulated great interest in understanding the nature of the catalytic activity, including the dependence on cluster size. The deposition of size-selected nanoclusters onto oxides has been recently employed by two groups to explore size-dependent chemical and physical properties of these systems. Heiz *et al.* showed that the catalytic activity of  $\text{Au}_n$  ( $n \leq 20$ ) on MgO (100) films in the oxidation of CO was highest for  $\text{Au}_{18}$  and that  $\text{Au}_8$  was the smallest cluster which exhibited catalytic behavior.<sup>5</sup> A similar investigation at room temperature involving  $\text{Au}_n$  ( $n = 1, 2, 3, 4, 7$ ) supported on rutile  $\text{TiO}_2$  (110) by Anderson *et al.* suggests a strong size-dependence in the oxidation of CO, with significant reactivity for clusters as small as  $\text{Au}_3$ .<sup>6</sup>

While these two studies show a strong dependence of the catalytic activity on the deposited cluster size, the size (and shape) of the metal clusters once they are deposited on the substrate was not measured directly in either case. It is well known from scanning tunneling microscopy (STM) images of evaporated Au and Ag, assumed to be monomeric in the vapor phase, that these metals sinter upon reaching the surface of  $\text{TiO}_2$  to form larger clusters ( $\geq 10$  atoms).<sup>7-10</sup> This underscores the importance of directly probing the cluster size distribution that results from the deposition of mass-selected clusters at room temperature.

In experiments described here we have imaged, using STM, the size and shape of Ag nanoclusters resulting from

the deposition of size-selected  $\text{Ag}_n^+$  clusters ( $n=1, 2, 3$ ) deposited at room temperature on single crystal rutile  $\text{TiO}_2$  (110)-(1×1) in UHV under conditions of soft landing ( $< 2$  eV per atom). Size distributions of clusters on the surface will be measured as a function of the size of the deposited cluster. Location of the clusters will also be explained.

## EXPERIMENT

The  $\text{Ag}_n^+$  clusters are produced in a laser ablation source, which is described in detail elsewhere.<sup>11</sup> A typical mass spectrum obtained from the cluster source is shown in Fig. 1(a). Intense beams of  $\text{Ag}_1^+ - \text{Ag}_3^+$  are obtained, which are used in the experiments described here. To create these clusters, a 50 Hz pulsed YAG laser beam (532 nm, 500 mJ/pulse max power) is focused on a rotating, translating silver rod. Prior to the laser pulse, a pulse of argon enters the source cavity and nucleation occurs. Positive ions are extracted from the source and the clusters are accelerated through a skimmer, focused via ion optics, and are further accelerated into a magnet where the mass-selection occurs. The energy spread of the beam of mass-selected ions is determined by measuring the current as a function of applied positive voltage on a detector placed in the beam path following the magnet. The full-width half-maximum (FWHM) energy spread of the beam was measured at the movable detector to be 2, 4, and 10 eV for the monomer, dimer, and trimer, respectively. A typical energy spread is shown for the monomer in Fig. 1(b). To deposit clusters this ion detector is removed from the beam path and the mass-selected clusters enter the UHV deposition chamber (base pressure  $< 1 \times 10^{-9}$  Torr). The beam is focused on another detector directly in front of the sample, where the deposition flux is measured and opti-

<sup>a)</sup>Corresponding author. Electronic mail: buratto@chem.ucsb.edu

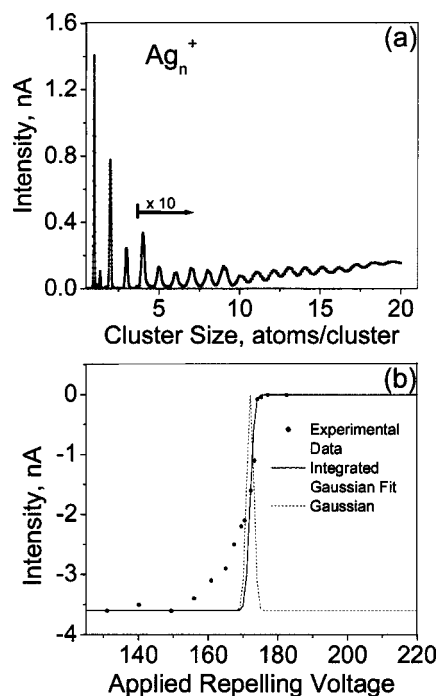


FIG. 1. (a) Mass spectrum of  $\text{Ag}_n^+$  clusters produced with a laser ablation source. Note: the peak present between  $\text{Ag}_1$  and  $\text{Ag}_2$  is likely  $\text{AgAr}^+$ , which results from the high pressure of argon present in the source chamber. (b) Sample kinetic energy distribution of the Ag monomer. The voltage is varied on the detector while measuring the ion current on the detector placed in the path of the ion beam. During deposition, the sample is biased at the midpoint of the distribution, therefore only clusters with kinetic energy greater than the midpoint (172 eV) are deposited. We use an integrated Gaussian trace to fit the high-energy side of the data, which differentiates to give a Gaussian distribution with a full width half maximum value of 2 eV. The majority of the monomers therefore arrive with an energy spread of half of this value, 1 eV.

mized. This detector is removed during deposition on the single crystal rutile  $\text{TiO}_2$  (110) sample. The sample is positively biased at the midpoint kinetic energy of the distribution ( $\sim 175$  eV) in order to soft-land the clusters ( $\sim 2$  eV/atom).

A beam intensity of  $\sim 1$  nA/cm<sup>2</sup> was typical. Deposition times were set to obtain  $\sim 2 \times 10^{13}$  Ag atoms/cm<sup>2</sup>, which is equivalent to 1.5% of a close packed silver monolayer. Prior to cluster deposition, the titania samples (Commercial Crystal Laboratories) were cleaned in UHV with cycles of argon bombardment (0.5–1 keV) and annealing to 860 K, consistent with published preparation methods for rutile titania (1  $\times$  1).<sup>12</sup> After cluster deposition the sample was translated under vacuum into a separate chamber in which the base pressure was  $< 3 \times 10^{-10}$  Torr, and imaged using STM. STM images of the surface were acquired at room temperature on an RHK SPM100 instrument with typical operating parameters of +1 to +2 V sample bias and tunneling current of 0.1 to 0.2 nA.

## RESULTS AND DISCUSSION

Figure 2 shows an STM image ( $1000 \text{ \AA} \times 1000 \text{ \AA}$ ) of a clean  $\text{TiO}_2$  (110)-(1  $\times$  1) substrate consisting of terraces  $\sim 400 \text{ \AA}$  wide and steps  $\sim 3.2 \text{ \AA}$  high, the latter of which is in agreement with the expected step height for the rutile

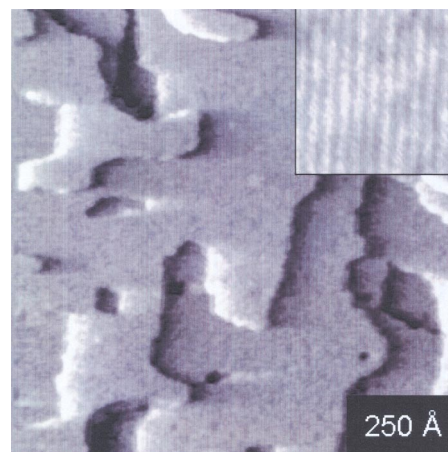


FIG. 2. An STM image ( $1000 \text{ \AA} \times 1000 \text{ \AA}$ ) of the clean titania surface. The inset is a high resolution image ( $62 \text{ \AA} \times 62 \text{ \AA}$ ) which shows the five-fold coordinated titanium (bright) and bridging oxygen rows (dark).

(110)-(1  $\times$  1) surface.<sup>13</sup> A high-resolution image of the surface is shown in the inset of Fig. 2. The alternating bright and dark lines have been assigned in the literature to five-fold coordinated titanium atom rows, and bridging oxygen atom rows, respectively. They are separated by  $6.5 \text{ \AA}$ , in agreement with the value predicted by the rutile structure.<sup>14</sup> Although the measurements reported here were taken from three different crystals, preparation methods were such that similar terrace widths were obtained in all cases. In some cases a low density (covering  $< 1\%$  of the surface) of small strands, with heights of  $1.8 \text{ \AA}$  were observed. These features have been attributed to a 1  $\times$  2 reconstruction of the surface.<sup>15</sup> They had no apparent effect on the results presented here.

Figure 3 shows an image after deposition of Ag monomers. Only large, cluster-like features are observed, consistent with the formation of three-dimensional (3-D) islands.<sup>8,9</sup> These islands average  $7.5 \text{ \AA}$  in height and  $42 \text{ \AA}$  in width measured at the base of the cluster, corresponding to a structure which is two to three atoms tall, containing approximately 50 atoms. It is possible to determine the surface cov-

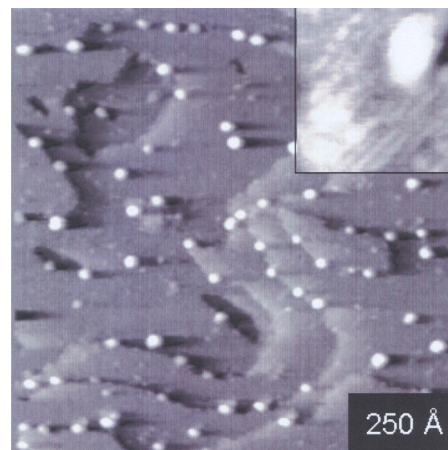


FIG. 3. An STM image ( $1000 \text{ \AA} \times 1000 \text{ \AA}$ ) of the titania surface after the deposition of 0.03 ML of Ag monomers. The monomers nucleate into larger clusters, many of which are located at step edges. The inset image ( $77 \text{ \AA} \times 77 \text{ \AA}$ ) shows a clean terrace area beside a large cluster.

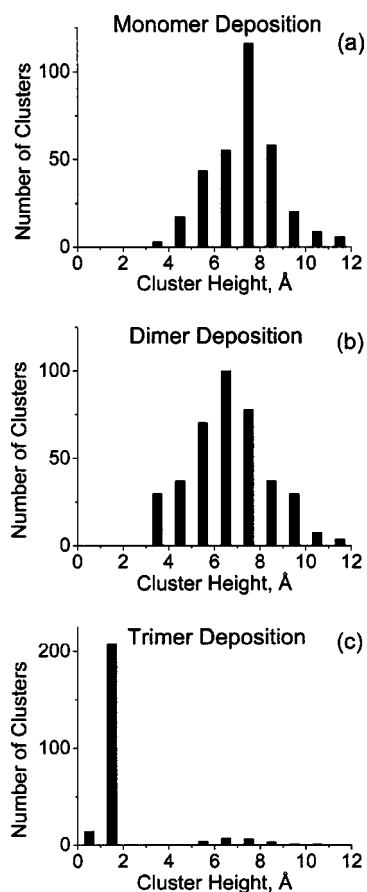


FIG. 4. Cluster height distributions for (a) the monomer, (b) the dimer, and (c) the trimer depositions. The data in each graph is averaged over several images, and representative of the number of clusters found in an area of  $2000^2 \text{ \AA}^2$ . Monomer and dimer distributions are similar, with a slight shift to smaller average cluster size in the case of the dimer. The trimer distribution shows a narrow peak in the size range of 1 to 2 Å in height, indicating that these features are true trimers.

erage from an average of STM images of the type shown in Fig. 3. It is important to note, however, that the observed width of each island is an overestimation due to the convolution of the tip with the nanocluster and is therefore not used in the calculation of the surface coverage. Instead, the clusters are approximated to be hemispherical in shape with a radius equal to the measured height, and are assumed to have an inter-atom distance equal to that of bulk Ag (2.9 Å), yielding a coverage of 0.03 ML. This coverage estimate is approximately a factor of two higher than the coverage predicted from the ion current, which is a reasonable agreement given the assumptions involved. A histogram of cluster heights averaged over several images is given in Fig. 4. A near gaussian cluster height distribution is obtained yielding an average height of 7.5 Å and a standard deviation of 1.5 Å for the monomer as shown in (a). We have obtained a similar distribution in previous experiments where silver was evaporated onto  $\text{TiO}_2$  using a resistively heated doser.<sup>10</sup>

The sintered clusters prefer to nucleate at step edges, a phenomenon also observed previously in the evaporation of Ag onto titania.<sup>8,10</sup> Close examination of the substrate between the Ag clusters, as shown in Fig. 3(b), reveals clean rows of five-coordinate titanium atoms and bridging O atoms. These findings confirm that size-selected silver mono-

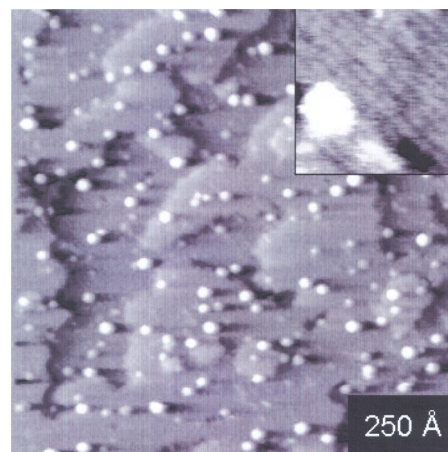


FIG. 5. An STM image ( $1000 \text{ \AA} \times 1000 \text{ \AA}$ ) of the titania surface after the deposition of 0.02 ML of Ag dimers. The dimers nucleate into larger clusters, some of which are located at step sites. The inset image ( $72 \text{ \AA} \times 72 \text{ \AA}$ ) shows the clean rows of titanium and bridging oxygen atoms between the larger clusters.

mers are highly mobile on the titania surface, and establish a minimum diffusion length of 200 Å, half of the average terrace width of 400 Å.

Figure 5 shows a large scale STM image taken after the deposition of silver dimers with a coverage of  $\sim 0.02$  ML. 3-D islands are visible with a cluster size distribution [Fig. 4(b)] similar to that obtained from the deposition of Ag monomers. The cluster heights and widths average 6.2 Å and 33 Å, respectively, both smaller than the monomer values. This implies the cluster size is smaller for deposition of dimers. Since the total coverage is approximately the same as in monomer deposition, dimer deposition results in approximately 20% higher cluster density.

There are noticeably fewer clusters at the step edge in the dimer deposition than in the monomer deposition; a step to terrace ratio of  $175 \pm 55$  (175:1) is obtained for the monomer deposition, and  $62 \pm 42$  for the dimer case. These results suggest the diffusion length of the dimer is smaller than that of the monomer and that the dimer is not able to reach as many step sites as the monomer, resulting in more clusters on the terraces.

Figure 6 shows an STM image taken after the deposition of trimers. The total metal deposited is once again the same as in the monomer and dimer depositions. It is clear from the image in Fig. 6 that far fewer large, sintered clusters appear than in the monomer and dimer depositions. Examination of the terrace areas between the large clusters in Fig. 6 reveals a high density of very small clusters that average 1.5 Å in height, 12 Å in width, and are thus only a few atoms in size. It is important to note here that the images do not change during several hours of scanning. These features, which we attribute to true trimers, are present on the sample at a coverage of 0.015 ML. The trimers appear predominantly at terrace sites, indicating that many of the initially deposited trimer clusters are immobile on the titania surface. Furthermore, the trimers are found mainly above the five-fold coordinated titanium atoms, as seen in the inset of Fig. 6. There is also a low density of large, sintered clusters that contributes an atomic coverage of 0.013 ML, bringing the



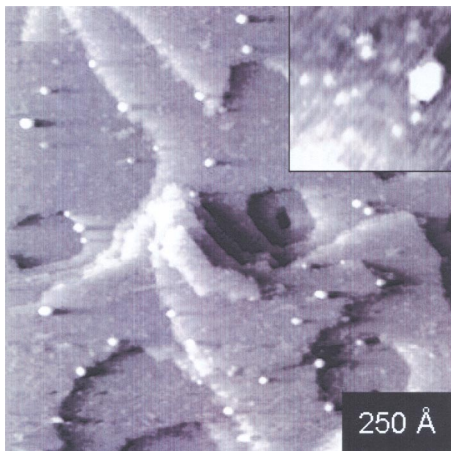


FIG. 6. An STM image ( $1000 \text{ \AA} \times 1000 \text{ \AA}$ ) of the titania surface after the deposition of 0.03 ML of Ag trimers. Fewer sintered clusters are observed; however, many atomic-sized features are seen on the surface as shown in the inset ( $69 \text{ \AA} \times 69 \text{ \AA}$ ).

total Ag coverage to 0.028 ML, approximately the same as in the monomer and dimer depositions. These larger clusters average  $6.8 \text{ \AA}$  in height and  $32 \text{ \AA}$  in diameter, and are observed mainly at step edges, with a step to terrace ratio of  $90 \pm 25$ . We attribute the fraction of monomers which nucleate into larger clusters to be mobile monomers and dimers resulting from the fragmentation of a fraction of the trimers.

## SUMMARY

Our investigation shows that the deposition of size-selected Ag clusters on rutile  $\text{TiO}_2$  (110)-(1  $\times$  1) results in a size distribution that depends strongly on the number of atoms in the deposited cluster. Silver monomers are highly mobile on the surface, forming large clusters that preferably

nucleate at step sites. Silver dimers are less mobile than monomers, but have enough mobility to form relatively large clusters that nucleate both at step and terrace sites. Silver trimers have very limited mobility on the surface, therefore remain as trimers, which nucleate predominantly on terrace sites.

## ACKNOWLEDGMENTS

This work was funded by the Air Force Office of Scientific Research under the DURINT program with grant number F49620-01-04J9. We would also like to acknowledge Manuel Manard for his assistance in the construction of the instrumentation.

- <sup>1</sup>M. Haruta, *Catal. Today* **36**, 153 (1997).
- <sup>2</sup>P. Claus and H. Hofmeister, *J. Phys. Chem. B* **103**, 2766 (1999).
- <sup>3</sup>W. Grunert, A. Bruckner, H. Hofmeister, and P. Claus, *J. Phys. Chem. B* **108**, 5709 (2004).
- <sup>4</sup>A. L. de Oliveira, A. Wolf, and F. Schuth, *Catal. Lett.* **73**, 157 (2001).
- <sup>5</sup>A. Sanchez, S. Abbet, U. Heiz, W. D. Schneider, H. Hakkinen, R. N. Barnett, and U. Landman, *J. Phys. Chem. A* **103**, 9573 (1999).
- <sup>6</sup>S. Lee, C. Fan, W. Tainpin, and S. L. Anderson, *J. Am. Chem. Soc.* **126**, 5682 (2004).
- <sup>7</sup>X. Lai, T. P. St. Clair, M. Valden, and D. W. Goodman, *Prog. Surf. Sci.* **59**, 25 (1998).
- <sup>8</sup>D. A. Chen, M. C. Bartelt, S. M. Seutter, and K. F. McCarty, *Surf. Sci.* **464**, L708 (2000).
- <sup>9</sup>D. Martin, F. Creuzet, J. Jupille, Y. Borensztein, and P. Gadenne, *Surf. Sci.* **377**, 958 (1997).
- <sup>10</sup>X. Tong, L. Benz, A. Kolmakov, S. Chretien, H. Metiu, and S. K. Buratto, *Surf. Sci.* **575**, 60 (2005).
- <sup>11</sup>P. K. Kemper and M. T. Bower (unpublished).
- <sup>12</sup>M. Li, W. Hebenstreit, L. Gross, U. Diebold, M. A. Henderson, D. R. Jennison, P. A. Schultz, and M. P. Sears, *Surf. Sci.* **437**, 173 (1999).
- <sup>13</sup>H. Onishi and Y. Iwasawa, *Surf. Sci.* **313**, L783 (1994).
- <sup>14</sup>U. Diebold, *Surf. Sci. Rep.* **48**, 53 (2003).
- <sup>15</sup>R. E. Tanner, M. R. Castell, and G. A. D. Briggs, *Surf. Sci.* **413**, 672 (1998).